JACS
JOURNAL OF THE AMERICAN CHEMICAL SOCIETY
Article
pubs.acs.org/JACS

Electrostatically Driven Second-Sphere Ligand Switch between High and Low Reorganization Energy Forms of Native Cytochrome *c*

Damián Alvarez-Paggi,[†,‡,#] María A. Castro,[†,‡,#] Verónica Tórtora,[§,⊥] Laura Castro,[§,⊥] Rafael Radi,[§,⊥] and Daniel H. Murgida*[,†,‡]

[†]Departamento de Química Inorgánica, Analítica y Química Física and [‡]INQUIMAE (CONICET-UBA), Facultad de Ciencias Exactas y Naturales, Universidad de Buenos Aires, Ciudad Universitaria, Pab. 2, piso 1, C1428EHA-Buenos Aires, Argentina

[§]Departamento de Bioquímica and [⊥]Center for Free Radical and Biomedical Research, Facultad de Medicina, Universidad de la República, Montevideo, Uruguay

Supporting Information

ABSTRACT: We have employed a combination of protein film voltammetry, time-resolved vibrational spectroelectrochemistry and molecular dynamics simulations to evaluate the electron-transfer reorganization free energy (λ) of cytochrome *c* (Cyt) in electrostatic complexes that mimic some basic features of protein−protein and protein−lipid interactions. The results reveal the existence of two native-like conformations of Cyt that present significantly different λ values. Conversion from the high to the low λ forms is triggered by electrostatic interactions, and involves the rupture of a weak H-bond between first- (M80) and second-sphere (Y67) ligands of the heme iron, as a distinctive feature of the conformational switch. The two flexible Ω loops operate as transducers of the electrostatic signal. This fine-tuning effect is abolished in the Y67F Cyt mutant, which presents a λ value similar to the WT protein in electrostatic complexes. We propose that interactions of Cyt with the natural redox partner proteins activate a similar mechanism to minimize the reorganization energy of interprotein electron transfer.

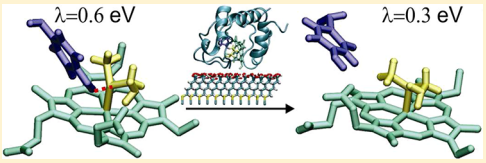

INTRODUCTION

Natural selection has evolved specialized redox proteins able to perform fast intra- and intermolecular long-range electron-transfer (ET) reactions, in the milliseconds time scale and below, despite involving nearly null thermodynamic driving forces.[1] Most of these nonadiabatic reactions are well described by the high temperature limit expression of Marcus semi-classical theory. Accordingly, the ET rate is proportional to the square of the electronic coupling matrix element, H_{DA}, that represents the electron tunneling probability between degenerate donnor and acceptor states, and to a Franck−Condon exponential term that acounts for the thermal accesibility of such degeneracy:[2]

$$k_{ET} = \frac{2\pi}{\hbar} |H_{DA}|^2 \frac{1}{\sqrt{4\pi\lambda k_B T}} \exp -\left(\frac{(\Delta G + \lambda)^2}{4\lambda k_B T}\right) \quad (1)$$

The relevance of the structural details and fluctuations of the protein bridging the two redox centers in modulating H_{DA} has been extensively and controversially discussed, concluding that resonant electron tunneling is greatly facilitated by the protein matrix.[1,3−5] Another rate-accelerating mechanism evolved by nature is the ability of the protein and redox site structure to reduce the activation barrier ($\Delta G^{\ddagger}$) for achieving degeneracy of the electronic initial and final states of the reaction. Within Marcus approximation,[2] this term can be expressed as $\Delta G^{\ddagger} = (\Delta G + \lambda)^2/4\lambda$, where λ is the reorganization free energy required to distort the equilibrium nuclear configuration of reactants toward the equilibrium configuration of products before ET. λ can be divided into inner and outer sphere: λ_{in} and λ_{out}, respectively. For metalloproteins λ_{in} is mainly determined by redox-linked structural changes within the first coordination sphere, and thus it is minimized by rigid cofactors.[6] Rearrangements of the remainder of the protein and the environment are comprised in λ_{out}. Thus, it can be anticipated that λ_{out} is minimized by a rigid protein matrix that effectively shields the redox site from solvent water molecules. Indeed, it has been shown that reducing solvent accessibility to the redox site and to the protein surface lowers the value of λ.[7,8] Establishing the relative magnitudes and cut off between the λ_{in} and λ_{out} terms, however, is far from trivial. Even less established is the possible modulation of λ through mechanisms such as protein−protein interactions or transmembrane potentials able to affect structural and physicochemical parameters relevant to the ET reaction.[9−11] These issues are of utmost importance, for instance, for understanding the origin of fast ET reactions involved in biological electron−proton energy transduction.[12,13]

The relatively slow progress in this respect is mainly ascribable to inherent experimental difficulties for obtaining accurate direct determinations of λ, which results in a small number of systematic studies.[1,14] Quantitative calculations of λ by molecular dynamics (MD) and quantum mechanical methods also remain challenging and are often difficult to

Received: December 6, 2012
Published: March 4, 2013

 © 2013 American Chemical Society

validate, partially due to the scarce number of reliable experimental values.[6,9,11,15,16]

Cytochrome *c* (Cyt) is a multifunctional enzyme involved in several processes central to cell life and death, such as electron shuttling from cytochrome bc_1 (Cyt-bc_1) to the terminal oxygen reductase (CcO) in the mitochondrial electron transport chain. It is also involved in the generation and trapping of reactive oxygen species, binding and oxidation of cardiolipin in the early events of apoptosis and assembly of the apoptosome.[17] Due to its simplicity, stability and availability, Cyt represents a hallmark in protein ET research that has been investigated by a large variety of experimental and theoretical methods.[18] Yet, the variability of λ values estimated from theory and experiments is amazingly large, spanning a range from ca. 0.22 to 1.1 eV,[14,19−25] including some even more extreme values.[26]

In the present work we have employed a combination of protein film voltammetry (PFV), time-resolved vibrational spectroelectrochemistry and MD simulations to evaluate the reorganization energy of wild-type (WT) mammalian Cyt and selected mutants in model electrostatic complexes that mimic some basic features of the interactions of Cyt with its natural redox partners.[27] We identified two native-like Cyt states that do not differ significantly in terms of the heme pocket and secondary structure elements, but represent low and high reorganization energy forms, respectively. Interconversion between these two forms is electrostatically driven and includes the rupture of a weak hydrogen-bond between the first-sphere iron ligand methionine 80 (M80) and the second-sphere ligand tyrosine 67 (Y67) as a key distinctive feature. The results provide a consistent way for rationalizing the broad range of λ values previously reported for cytochromes from different species based on the conservation of this critical H-bond. We propose that formation of electrostatic complexes of Cyt with its natural redox partners, Cyt-bc_1 and CcO, activates similar structural changes, thus accelerating interprotein ET reactions.

■ MATERIALS AND METHODS

Protein Preparation. Wild-type Cyt from horse heart was purchased from Sigma-Aldrich (C7752). WT_{rec} and Y67F were produced and purified as described elsewhere.[28,29] All protein variants were stored lyophilized and resuspended in a 12.5 mM phosphate, 12.5 mM sulfate buffer at pH 7 for all experimental determinations.

Resonance Raman. Resonance Raman (RR) spectra were recorded either with 413 nm (3 mW, Spectra-Physics BeamLok 2060) or 514 nm excitation (13 mW, Coherent Innova 70c) in backscattering geometry using a confocal microscope coupled to a single stage spectrograph (Jobin Yvon XY 800) equipped with a CCD detector. Protein samples (1 mM) were placed into a rotating quartz cell for the measurements.

Vibrational Spectroelectrochemistry. Stationary and time-resolved surface-enhanced resonance Raman (TR-SERR) determinations were performed using a three-electrode spectroelectrochemical cell mounted in front of the same spectrograph employed for RR measurements. The silver ring working electrode was mechanically polished and subjected to oxidation−reduction cycles in 0.1 M KCl to create SERR-active nanostructured surfaces and subsequently incubated in 1.5 mM ethanolic solutions of the alkanethiols (pure HS-$(CH_2)_{15}$-COOH or a 1:1 mixture of HS-$(CH_2)_{15}$-CH_2OH: HS-$(CH_2)_{15}$-COOH or 1:1) for ca. 24 h and transferred to the spectroelectrochemical cell. The SAM-coated silver ring was mounted on a shaft that is rotated at about 5 Hz to avoid laser-induced sample degradation. The electrode potential was controlled with a TeQ03 potentiostat. All potential cited in this work refer to the Ag/AgCl (3.5 M KCl) electrode. The spectroelectrochemical cell has been described in detail elsewhere.[30] For TR-SERR experiments, potential jumps of variable height and duration were applied to trigger the reaction. The SERR spectra were measured at different delay times following the potential jump. Synchronization of potential jumps and probe laser pulses was achieved by a pulse-delay generator (BNC). The probe pulses were generated by passing the cw laser beam through two consecutive laser intensity modulators (QIOPTICS Photonics), which give a total extinction better than 1:50000 and a time response of ca. 20 ns. Details may be found elsewhere.[31,32]

Electrochemical Determinations. PFV and cyclic voltammetry (CV) experiments in solution were perfomed with a Gamry REF600 potentiostat using a non-isothermal cell equipped with a polycrystalline gold bead working electrode, a Pt wire auxiliary electrode and a Ag/AgCl (3.5 M KCl) reference electrode to which all potentials in this work are referred. Au electrodes were first oxidized in 10% $HClO_4$ applying a 3 V potential for 2 min, sonicated in 10% HCl for 15 min, rinsed with water and subsequently treated with a 3:1 v/v H_2O_2:H_2SO_4 mixture at 120 °C. The electrodes were then subjected to repetitive voltammetric cycles between −0.2 and 1.6 V in 10% $HClO_4$ and thoroughly washed with water and ethanol. Au working electrodes were coated with self-assembled monolayers (SAMs) by overnight incubation in a 1 mM solution of the constituent alkanethiols: HS-$(CH_2)_5$-CH_2OH for CV experiments and a 1:1 mixture of HS-$(CH_2)_n$-CH_2OH:HS-$(CH_2)_n$-COOH of varying chain length for PFV.

CV determinations were performed in a 0.5 mM solution of Cyt, while for PFV experiments the SAM-coated gold electrodes were incubated for ca. 2 h in the Cyt solution, then carefully rinsed and inserted into the electrochemical cell. All electrochemical determinations were performed in phosphate/sulfate buffer 12.5:12.5 mM, pH 7. The dependence of the apparent rate constant k_{ET}^{app} on distance was determined through PFV recording the separation of the anodic and cathodic peaks as a function of the scan rate and using Laviron's working curve.[33]

Optical Spectroscopy. Electronic absorption spectra were acquired with a Thermo Scientific Evolution Array spectrophotometer using quartz cells of 1 cm optical path length.

Computational Methods. The starting structure for simulations of Cyt in the ferric state corresponds to the oxidized form of WT horse heart Cyt (PDB ID 1HRC).[34] Details for Cyt in the ferrous state are provided as Supporting Information (SI). The Y67F mutant was built *in silico* replacing the corresponding side chains and relaxing the resulting structure using classical MD. For simulating the SAMs, an infinite array of fixed Au atoms with lattice structure 111 was built *in silico*, and each of them was linked to either a C5-COOH or a C5-COO^- molecule through the S atom, the relative ammounts of each determining the protonation percentage of the SAM. Lattice and SAM parameters were adopted from the literature.[35] Details of the MD runs, the scoring function for the Y67-M80 H-bonding interaction, and the structural analysis of Cyt adsorbed on SAMs are described in the SI.

■ RESULTS AND DISCUSSION

Tyrosine 67 as Second-Sphere Ligand. Y67 has been proposed a key residue in controlling Cyt structure and function through a network of H-bonds.[36] However, interactions such as the H-bond between Y67 and M80 (Figure 1) are often assumed based on visual inspection of crystal structures and on extrapolation of indirect evidence obtained for Cyt variants from different organisms.[28,37−40] Recent MD simulations on human Cyt refute this interaction.[41] One should note, though, that the search parameters usually employed in these simulations are not optimized for H-bonds in which the acceptor is an S atom.[42] Therefore, to solve this controversy, we performed MD simulations of ferric Cyt in explicit solvent and evaluated the distances between the S_{M80} atom and the phenolic H_{Y67} and O_{Y67} atoms (*d* and *D*, respectively) and three characteristic angles: (i) between the bisector of the C^{γ}-S^{δ}-C^{ε} angle from M80 and the S_{M80}-H_{Y67} vector (ψ), (ii) between said bisector and the projection of the S_{M80}-H_{Y67} vector on the C^{γ}-

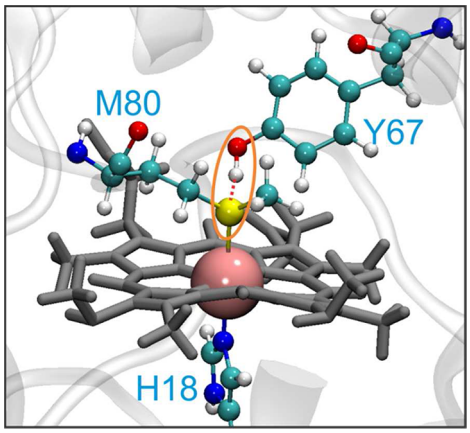

Figure 1. Detail of the redox center of Cyt. The heme iron is axially coordinated by residues histidine 18 (H18) and M80. Y67 is H-bonded to M80, thus constituting a second-sphere ligand.

S^{δ}-C^{ε} plane (φ), and (iii) the O_{Y67}-H_{Y67}-S_{M80} angle, as originally defined by Zhou et al. (Figure S1).[42] As shown in Figure 2, the average values adopted by the five parameters along the simulation are similar to the mean values proposed as optimal for H-bonding based on the analysis of 500 protein structures.[42] To facilitate the analysis, we designed a simple scoring algorithm that assigns 1 point whenever the calculated parameter lies within the optimal range (mean value ± SD). Thus, a scoring of 5 implies optimal H-bonding, while a value of 0 indicates no interaction. The last panel of Figure 2 shows that the scoring oscillates between 0 and 5 along the 5 ns simulation, with an average value of 3.3. These results indicate the existence of a labile H-bond between the Y67 and M80 residues, thereby rendering Y67 as a weak second-sphere ligand of the heme iron. Similar results were obtained for ferrous Cyt (SI). In order to characterize possible effects of this ligand on the ET dynamics of Cyt, we produced and studied a mutant protein in which Y67 is replaced by phenylalanine (Y67F), i.e., by a residue unable to act as H donor.

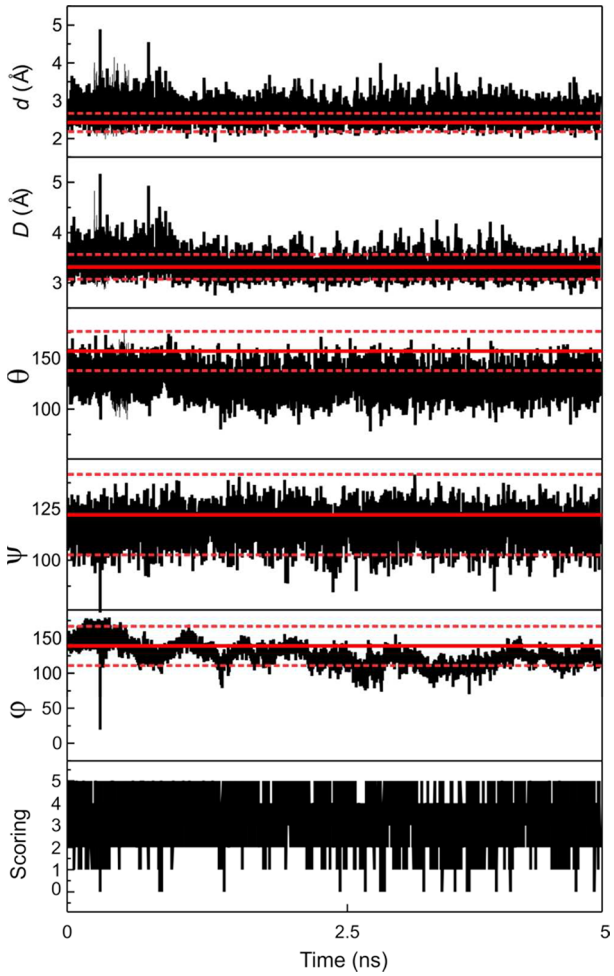

Figure 2. Structural parameters and scoring of the Y67-M80 H-bonding interaction as a function of MD simulation time for native ferric Cyt in explicit solvent. The red lines indicate mean values (continuous) and standard deviation (dotted) of the structural parameters adopted from Zhou et al. (Figure S1).[42] Similar results were obtained for ferrous Cyt (SI).

Characterization of the Protein Variants in Solution. The Y67F variant was produced including two additional modifications, H26N/H33N, for expression and purification purposes. Given that H26 and H33 are surface residues, these mutations are not expected to significantly affect the structure and redox properties of Cyt. As a control, we also produced the so-called WT recombinant protein (WT_{rec}), which only includes the H26N/H33N modifications.[29] UV−vis spectra of the two protein variants (Y67F and WT_{rec}) in the oxidized form are identical to WT Cyt. Spectra of WT and WT_{rec} in the reduced state are also undistinguishable, while Y67F presents a 2 nm red-shift of the Q bands, indicating only a small perturbation of the active site (Figure S2), in agreement with previous NMR studies.[28] This perturbation does not imply exchange of axial ligands and/or changes of the spin state of the heme iron, as resonance Raman (RR) spectra recorded under Soret- and Q-band excitation are almost identical for the three protein variants. Only minor differences of relative intensities of ferrous Y67F with respect to the WT species are observed (Figures 3 and S2). WT and WT_{rec} also exhibit nearly identical cyclic voltammetries in solution, thus confirming that the surface mutations do not affect the active site structure (Figures 4 and S3, and Table 1). In contrast, we notice some differences in the voltammetric response of Y67F, pointing out that interruption of the Y67-M80 H-bond influences the thermodynamic and kinetic redox parameters of Cyt. First, the standard reduction potential ($E°$) of Y67F is 40−50 mV lower than for WT and WT_{rec} proteins under identical conditions. A similar shift was reported for an equivalent mutant of yeast cytochrome *c* (iso-Cyt) that can be ascribed to (i) a diminished electron withdrawing power of Met 80 upon interruption of the Y67-M80 H-bond,[37] (ii) a change in the conformational polarizability of the protein matrix,[43] or (iii) an alteration of the internal electric fields that may perturb the heme group to different extents.[44] Second, the separations of the anodic and cathodic peaks of Y67F are significantly smaller than those observed for WT and WT_{rec} variants at similarly high scan rates (Figures 4). The latter result is indicative of faster heterogeneous ET of Y67F, which in principle can be rationalized either in terms of lower reorganization energy (λ) or of higher electronic coupling (H_{DA}) compared to the WT proteins.

Characterization of the Protein Variants in Electrostatic Complexes. It has been shown in previous work that the basic features of the electrostatic interactions between Cyt and its natural redox partners Cyt-bc_1 and CcO, can be mimicked using metal electrodes coated with self-assembled

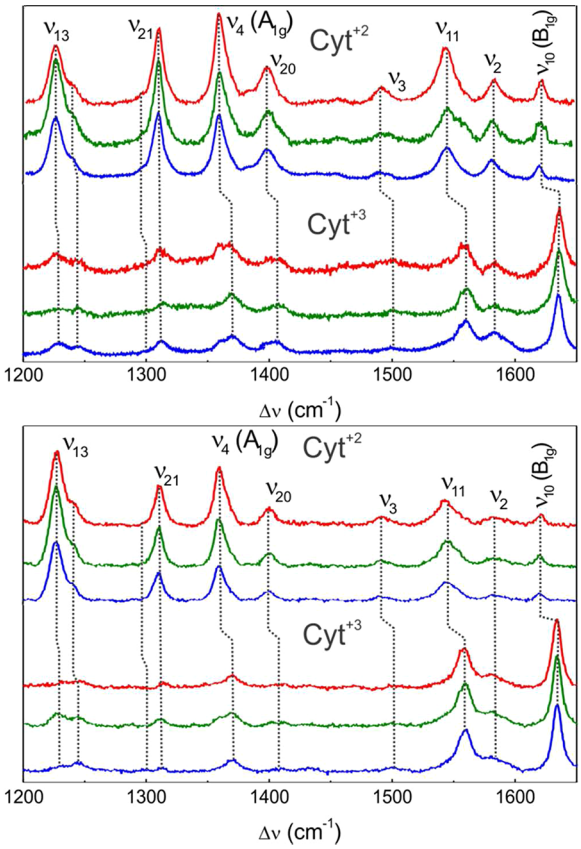

Figure 3. RR (top) and SERR (bottom) spectra of ferrous (Cyt^{+2}) and ferric (Cyt^{+3}) Cyt variants measured in solution and adsorbed on C10-COOH:C10-CH_2OH SAM-coated electrodes, respectively. Blue, WT; green, WT_{rec}; red, Y67F. All the spectra were recorded using 514 nm excitation.

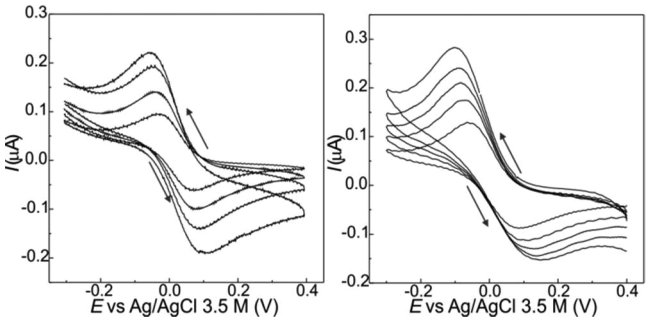

Figure 4. Selected CVs of the Y67F mutant (left) and WT_{rec} protein (right) measured in solution as a function of the scan rate under otherwise identical conditions. The arrows indicate the shifts in peak potentials and rising currents with increasing scan rates from 0.1 to 2 V s^{-1}.

Table 1. E^0 for Cyt Variants in Solution Obtained by Cyclic Voltammetry (CV Sol.) or Adsorbed on C10-COOH: C10-CH_2OH SAMs Determined by Either PFV or SERR

	E^0 (mV)		
	SERR	CV sol.	PFV
WT	12 ± 3	38 ± 12	1 ± 2
WT_{rec}	15 ± 2	49 ± 13	4 ± 2
Y67F	−34 ± 2	16 ± 1	−38 ± 5

monolayers (SAMs) of ω-carboxyl alkanethiols.[27] Here we have employed these model systems to address the relevance of electrostatic interactions in determining the redox properties of WT, WT_{rec} and Y67F Cyt variants. Specifically, two types of coatings were employed: (i) single-component SAMs of HS-$(CH_2)_n$-COOH (C*n*-COOH) with *n* = 5, 10, and 15, and (ii) 1:1 mixtures of HS-$(CH_2)_n$-COOH and HS-$(CH_2)_n$-CH_2OH (C*n*-COOH:C*n*-CH_2OH), in which the excess of surface negative charges provided by the carboxylate groups is diluted.

The integrity of the adsorbed proteins was investigated by SERR spectroelectrochemistry recorded under Soret-band excitation, which has proven to be very sensitive to changes of the redox state, coordination pattern and spin of the heme iron.[45] Spectra were recorded both at oxidizing and reducing applied electrode potentials for the three proteins adsorbed on the two types of SAMs. In all cases SERR spectra were essentially identical to the RR spectra of the corresponding ferric and ferrous forms in solution (Figure S4), thus indicating that the adsorbed species are electrochemically active and that the structure of the heme pocket is preserved upon immobilization.

Similar conclusions can be extracted from the comparison of positions and widths of SERR and RR bands measured under Q-band excitation (Figure 3). Note, however, that in this case the relative intensities of SERR and RR bands differ substantially. These results indicate that the orientation of the adsorbed species is largely homogeneous, as vibrational modes of different symmetry experience differential surface enhancements depending on the relative orientations of the electric field vector and the individual components of the scattering tensor.[46] Moreover, SERR spectra of Y67F and WT_{rec} measured at 514 nm are identical, and present only minor differences with respect to WT in terms of relative intensities of modes of different symmetry. Therefore, it can be concluded that the H26N/H33N mutations result only in a slightly different average orientation of the protein in the biomimetic complexes, and that the additional mutation of Y67 exerts no further influence. Based on these results, electronic couplings of immobilized WT_{rec} and Y67F with the metal electrode are anticipated to be similar, and to differ only slightly from WT.

PFV and SERR experiments reveal reversible electrochemical responses for the three protein variants in the electrostatic complexes (Figure 5). In agreement with measurements in solution, $E°$ values determined by the two methods are identical for WT and WT_{rec}, while the value for Y67F is down-shifted by ca. 40−50 mV (Table 1), thus confirming the structural integrity of the adsorbed proteins. The small differences observed between species adsorbed and in solution can be ascribed either to the interfacial potential drop across the SAMs[30] or to electrostatic interactions between the protein and the anionic surface.[47]

Electron-Transfer Dynamics of WT Cyt and Mutants in Electrostatic Complexes. Apparent rate constants of the heterogeneous ET reactions (k_{ET}^{app}) were determined by PFV using Laviron's working curve (Figure S5)[33] and by TR-SERR spectroelectrochemistry.[45] Control experiments for the three Cyt variants adsorbed on electrodes coated with SAMs of different composition and thickness yield the expected exponential increase of k_{ET}^{app} upon decreasing the SAM length (Table S1), consistent with the average tunneling decay β = 1.1/CH_2 reported previously.[48−50] Moreover, in the three cases k_{ET}^{app} levels off at sufficiently thin films, in agreement with previous observations for WT Cyt.[32] The origin of this plateau

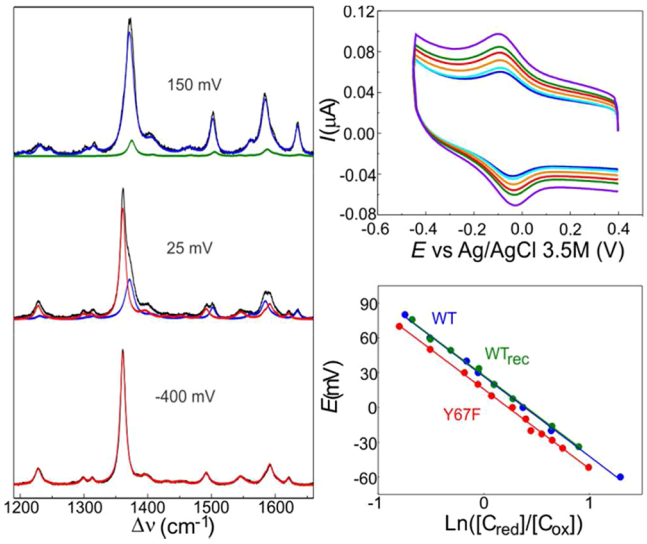

Figure 5. Left: SERR spectra (413 nm excitation) of WT Cyt adsorbed on C10-COOH:C10-CH_2OH SAM-coated Ag electrodes measured at different potentials (black). Relative concentrations were obtained by component analysis of reduced (red) oxidized (blue), and non-native forms (green).[45] Right top: Selected PFVs for Y67F adsorbed on C10-COOH:C10-CH_2OH SAM-coated Au electrodes recorded at increasing scan rates. Right bottom: Nernstian plots from the SERR spectra for the redox processes of WT (blue), WT_{rec} (green), and Y67F (red).

has been discussed in detail elsewhere.[8,27,46] It was concluded that, for WT Cyt at thicker SAMs, measured rates are determined by electron tunneling probability, while at thinner films protein and interfacial water dynamics become rate-limiting. Most likely, the same explanation holds for the WT_{rec} and Y67F variants and, therefore, we focused on the characterization of the three proteins adsorbed on C15-COOH SAMs, i.e., under conditions where the measured k_{ET}^{app} corresponds to a true ET process. The value of k_{ET}^{app} determined on these SAMs at zero driving force is almost 1 order of magnitude larger for Y67F than for WT_{rec} (Table S1). Such difference cannot be ascribed to different orientations as Q-band SERR spectra of these species are identical (see above). Instead, the most likely explanation is a lower reorganization energy (λ) of Y67F. For the WT and WT_{rec} proteins k_{ET}^{app} values differ by less than a factor of 2, which is consistent with slightly different orientations, as judged from the Q-band SERR spectra.

λ was determined for the different Cyt variants adsorbed on single-component (C15-COOH) and on mixed SAMs (1:1 C15-COOH:C15-CH_2OH) by TR-SERR. In these experiments k_{ET}^{app} was measured at constant temperature (298 K) by applying variable potential steps that represent increasing overpotentials for reduction ($\eta = E_f - E^\circ$). SERR spectra recorded as a function of time could be quantitatively simulated with variable proportions of native ferrous and ferric Cyt yielding in all cases monoexponential concentration profiles (Figures S6−S9). As shown in Figures 6 and S10, the rate constants obtained as a function of η exhibit the sigmoidal behavior predicted by theory for metal electrodes as described by eq 2:[51]

$$k_{ET}(\eta) = \frac{2\pi}{\hbar}|H|^2 \int_{\infty}^{-\infty} \frac{1}{1+\exp\left(\frac{\varepsilon-\varepsilon_f}{k_B T}\right)}\rho(\varepsilon) \frac{1}{\sqrt{4\pi\lambda k_B T}} \exp\left[-\frac{(\lambda - e\eta + \varepsilon)^2}{4\lambda k_B T}\right] \quad (2)$$

λ values summarized in Table 2 were obtained by fitting the experimental data presented in Figures 6 and S10 to the following simplified version of eq 2:[22]

$$k_{ET}(\eta) \approx \frac{\pi}{\hbar}|H_{DA}|^2 \operatorname{erfc}\left(\frac{\lambda + e\eta}{\sqrt{4\lambda k_B T}}\right) \quad (3)$$

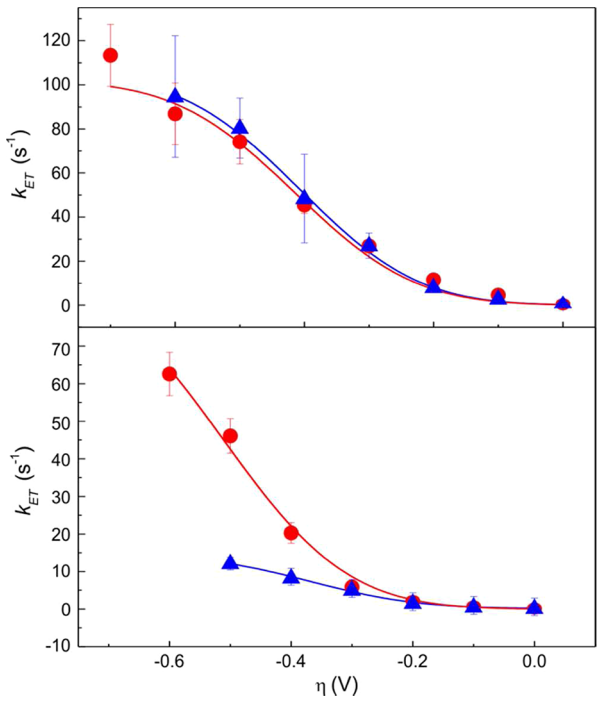

Figure 6. ET rate constants as a function of the overpotential for Y67F (top) and Cyt WT (bottom) adsorbed on C15-COOH SAMs (blue) and on 1:1 C15-COOH:C15-CH2OH SAMs (red). Results obtained from WTrec are identical to those from Cyt WT (Figure S10).

For both WT and WT_{rec} adsorbed on C15-COOH SAMs we obtain λ = 0.37 eV, which is very close to values determined previously under comparable conditions.[22,24,52] On mixed SAMs, however, this value increases by at least 40% to λ = 0.51 eV, which constitutes a lower limit estimate as the reductive desorption of the SAMs prevents application of larger overpotentials. Consistently, Arrhenius plots obtained by independent PFV determinations of k_{ET}^0 as a function of temperature performed under otherwise identical conditions, yielded λ = 0.6 eV for both WT and WT_{rec} proteins (Figure 7). The impact of increasing charge density on λ is consistent with previous reports.[53]

Maximum rate constants (k_{ET}^{max}) achieved at high overpotentials (Figure 6) are approximately 6 times larger on mixed SAMs compared to single-component C15-COOH films. Such increase corresponds to ca. 2 times larger electronic coupling, as determined by fitting the data with eq 2 and adopting the λ values obtained from eq 3 (Table 2). As shown in previous

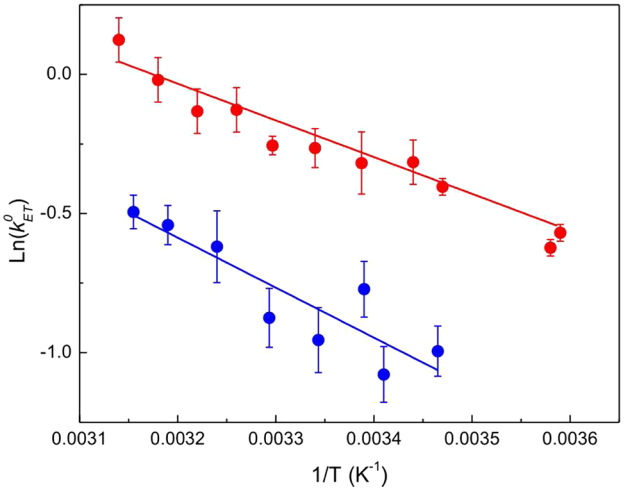

Figure 7. Temperature dependence of k^0_{ET} determined through PFV of adsorbed species on C15-COOH:C15-CH2OH SAMs for WT (blue) and Y67F (red). Reorganization energy values of 0.6 ± 0.1 eV and 0.45 ± 0.05 eV were obtained for Cyt WT and the Y67F mutant, respectively.

Table 2. Electron-Transfer Parameters of Cyt Variants Adsorbed on SAM-Coated Electrodes[a]

	k^0_{ET} (s^{-1})	k^{max}_{ET} (s^{-1})	λ (eV)	$\lvert H_{DA}\rvert$ (eV)
		WT		
		1:1 C15-COOH:C15-CH_2OH SAMs		
expt	0.17 ± 0.05	90 ± 10	0.51 ± 0.03	–
calcd	0.11	87.84	0.51	9.60×10^{-8}
		C15-COOH SAMs		
expt	0.24 ± 0.03	14 ± 1	0.37 ± 0.02	–
calcd	0.18	14.37	0.37	3.88×10^{-8}
		Y67F		
		1:1 C15-COOH:C15-CH_2OH SAMs		
expt	0.46 ± 0.03	101 ± 6	0.41 ± 0.03	–
calcd	0.37	101.84	0.41	1.03×10^{-7}
		C15-COOH SAMs		
expt	0.59 ± 0.03	100 ± 10	0.41 ± 0.03	–
calcd	0.4	109.8	0.41	1.07×10^{-7}

[a]Experimental values were obtained by adjusting the data presented in Figure 5 with eq 3. Calculated values were determined by simulating the same data set with eq 2 and adopting the λ values obtained from the fittings to eq 3.

work,[27] variations of H_{DA} of adsorbed WT Cyt by a factor of 2 are ascribable to only minor differences in the average position of surface side chains or very small coarse reorientations that can be expected due to slightly different interactions of the protein with the two SAMs. In agreement with this interpretation, relative intensities of SERR spectra recorded at 514 nm excitation on the two films exhibit only marginal differences within experimental error.

In sharp contrast, k_{ET} versus η curves obtained for Y67F are completely insensitive to the chemical composition of the SAM (Figure 6), yielding λ = 0.41 eV in both cases, i.e. very close to the value obtained for WT and WT_{rec} on C15-COOH SAMs. A very similar value (λ = 0.45 eV) is obtained from the temperature-dependence of k^0_{ET} as determined by PFV (Figure 7). The MD simulations predict that the dipole moment of Y67F is 15% larger than that of Cyt, suggesting a possible explanation for both the similarity between the k_{ET} versus η curves for Y67F on both SAMs and the differences in k^{max}_{ET} for Cyt WT. We ascribe these results to changes in H_{DA} since its value is strongly affected by the average coarse orientation of the protein (see above), which in turn depends on the interaction between the interfacial electric field and the dipole moment.

Taken together with the characterization of the complexes presented in the previous sections, these results suggest the existence of two alternative native-like conformations of Cyt with high and low reorganization energies, respectively. Conversion from the high λ to the low λ form appears to be triggered by electrostatic interactions. Most likely, the conformational transition involves the rupture of the H-bond between Y67 and M80 residues, as suggested by the similarity of λ values determined for Y67F and for the two WT forms in electrostatic complexes with the SAMs of higher charge density.

Structural Differences of Native Cyt Forms with Low and High λ Values. The spectral identity and the similar $E°$ values between Cyt species in solution and in complexes with SAMs show that the structure of the heme pocket and, most likely, also the entire native protein folding is largely preserved upon adsorption. Therefore, the switch between the high and low λ forms of WT Cyt in electrostatic complexes should reside in spectroscopically silent subtle conformational changes driven by electrostatic interactions.

In order to address the structural basis of this fine-tuning mechanism, we performed 5 ns MD simulations of WT ferric Cyt adsorbed on carboxyl-terminated SAMs with 10% ($SAM_{10\%}$), 25% ($SAM_{25\%}$), and 50% ($SAM_{50\%}$) deprotonation degrees, which provide a systematic way of analyzing possible conformational changes of Cyt as a function of the charge density of the SAMs. The initial structure and orientation of Cyt on the SAMs was adopted from previous work,[27] and presented a stable H-bond between Y67 and M80 with a scoring factor of 5.

The simulations show that the secondary structure elements and RMSD values of Cyt adsorbed on $SAM_{10\%}$ remain nearly identical to the protein in solution (Figure S11), although the average scoring factor for the Y67/M80 H-bond decreases to 3.1 (Figure 8). Also for Cyt/$SAM_{25\%}$ complexes the secondary structure elements remain nearly unaltered (Figure S12), although the RMSD increases in segments corresponding to

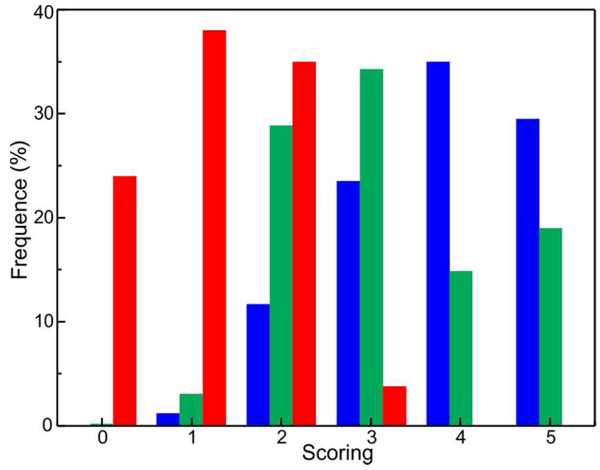

Figure 8. H-bond scoring distribution for WT ferric Cyt adsorbed on $SAM_{10\%}$ (blue), $SAM_{25\%}$ (green) and $SAM_{50\%}$ (red) obtained from 5 ns MD simulations.

two well-defined Ω loops (residues 20−30 and 70−85, Figure S13).[54] These results are in remarkably good agreement with those obtained upon formation of the iso-1-Cyt/cytochrome bc_1 complex,[55] where it was found that the Ω loop containing residues 25−30 is the most susceptible to structural variations. We found that the aforementioned changes result in a variation of both the average value and the distribution of the H-bond score (Figure 8). As expected, the effect is significantly more pronounced for Cyt/$SAM_{50\%}$ complexes, and the correlation between RMSD values and SAM protonation percentage is similar to that found in previous computational studies (Table S2).[56] Weakening of the H-bond appears to be independent of the redox state of Cyt (Figure S14), thus suggesting a predominant role of small collective structural perturbations of the protein matrix. Moreover, the presence of internal water molecules that participate in a network of H-bonding interactions that include the Y67 residue seems to exert a negligible impact on the liability of the H-bonding interaction (Figure S15).

One should note that the Ω loops that undergo deformations contain the majority of the lysine residues involved in establishing electrostatic contacts with the SAMs and with the natural redox partners of Cyt, such as mitochondrial complexes III and IV and cytochrome *c* peroxidase.[57−59] Remarkably, per residue RMSDs of Cyt adsorbed on $SAM_{10\%}$ are similar to those of Y67F in solution (Figure S12), thus suggesting that this mutation and electrostatic interactions trigger similar conformational transitions of Cyt. Therefore, we propose that the Y67/M80 H-bond is a key constituent of the conformational change between the high and low λ forms of Cyt, and that this switch is activated upon specific electrostatic interactions. It is important to remark that we do not ascribe the variation in λ to the disruption of the H-bond *per se*; more likely, this is a result of the collective perturbation of the dynamics and average position of the aminoacidic residues and nearby water molecules. We propose that this collective structural and dynamical change is achievable both through the disruption of the Y67-M80 H-bond and from electrostatic complex formation (that in turn weaken said H-bond, as shown above).

■ CONCLUSIONS

Recent nuclear resonance vibrational spectroscopy studies have demonstrated a dynamic link between the heme iron and the surface binding site of Cyt, which suggest that protein−protein interactions could eventually minimize λ.[60] The present results demonstrate that interruption of the Y67-M80 H-bond achieved either by Y67F mutation or by interactions of Cyt in electrostatic complexes do actually minimize λ to similar extents, thus underlying the involvement of this relatively weak interaction between first- and second-sphere ligands in stabilizing the high λ form. The conformational change between the high and low λ forms of Cyt is activated by deformations of the flexible Ω loops that contain most of the lysine residues which constitute the protein binding site. We propose that a similar mechanism could be triggered upon interactions of Cyt with the natural redox partners, CcO and Cyt-bc1, thus minimizing the reorganization energy for interprotein ET. Indeed, the interactions between Cyt and natural partner proteins involve the same lysine residues implicated in the model electrostatic complexes.[27,57,58,61]

These findings allow rationalizing the dispersion of λ values previously reported for cytochromes from different organisms. Equine, tuna, and yeast cytochromes all present weak H-bonds between a tyrosine residue and the axial ligand methionine that could be perturbed electrostatically. The average value of λ obtained for these proteins in solution is ca. 0.6 eV, but it reduces to ca. 0.3 eV in electrostatic complexes (Table 3). Moreover, cytochrome c_{551} from *P. aeruginosa* presents a λ value of 0.4 eV in solution, coincidentally with the lack of an equivalent H-bonding interaction.[66]

Table 3. Reorganization Energy Values Reported for Cytochromes from Different Organisms

protein	exptl conditions[a]	λ (eV)
Cyt horse heart	sol.	0.58[25]
	sol.	0.52[23]
	sol.	0.6[21]
	sol.	0.8[14]
	sol. (comp.)	0.69[19]
	ads. SC-SAMs	0.28[22]
	ads. SC-SAMs	0.35[24]
	ads. M-SAMs	0.7[20]
	sol. (urea, pH 7)	0.82[23]
	sol. (urea, pH 2)	0.41[21]
	coord. Py	0.50[62]
iso-Cyt	sol.	0.61[25]
	sol. (comp.)	0.77[63]
	ads.	0.35[64]
	ads. mutants	0.25−0.47[64]
Cyt tuna	sol.	0.62[25]
Cyt c_{551} *P. aeruginosa*	sol.	0.38[65]

[a]Abbreviations: comp., computational determinations; sol., experimental determinations in solution; ads., experimental determinations of adsorbed species; coord. Py, the heme iron is coordinated through the terminal pyridine of the SAMs; SC-SAMs, single-component C*n*-COOH SAMs; M-SAMs, mixed C*n*-COOH:C*n*-CH_2OH SAMs.

Electrostatic interactions and homogeneous electric fields have been recently shown to control the structure, electronic coupling, protein dynamics and even the nature of the redox active molecular orbitals involved in ET reactions of Cyt and Cu_A centers.[27,45,67,68] Thus, the fine-tuning of λ can be envisaged into a broader context of regulation of biological electron−proton energy transduction through specific interactions and transient changes of the membrane potential.

■ ASSOCIATED CONTENT

Supporting Information

Computational methods; additional spectroscopic, spectroelectrochemical, and electrochemical data; and MD simulation results. This material is available free of charge via the Internet at http://pubs.acs.org.

■ AUTHOR INFORMATION

Corresponding Author

dhmurgida@qi.fcen.uba.ar

Author Contributions

[#]D.A.-P. and M.A.C. contributed equally.

Notes

The authors declare no competing financial interest.

ACKNOWLEDGMENTS

Financial support from ANPCyT (PICT 2010-070 and 2011-1249) and UBACyT to D.H.M., from ANII (FCE 2486) and CSIC-UdelaR to R.R., and from Centro de Biología Estructural del Mercosur (CeBEM) to both groups is gratefully acknowledged. This research was partially done using resources provided by the Open Science Grid, which is supported by the National Science Foundation and the U.S. Department of Energy's Office of Science. D.A.-P. and M.A.C. thank CONICET for fellowships. V.T. was partially supported by a fellowship from ANII. D.H.M. is staff member of CONICET.

REFERENCES

(1) Moser, C. C.; Keske, J. M.; Warncke, K.; Farid, R. S.; Dutton, P. L. *Nature* **1992**, *355*, 796−802.
(2) Marcus, R. A. *J. Chem. Phys.* **1956**, *24*, 966−978.
(3) Balabin, I. A.; Beratan, D. N.; Skourtis, S. S. *Phys. Rev. Lett.* **2008**, *101*, 158102−158105.
(4) Beratan, D. N.; Betts, J. N.; Onuchic, J. N. *Science* **1991**, *252*, 1285−1288.
(5) Gray, H. B.; Winkler, J. R. *Proc. Natl. Acad. Sci. U.S.A.* **2005**, *102*, 3534−3539.
(6) Sigfridsson, E.; Olsson, M. H. M.; Ryde, U. *J. Phys. Chem. B* **2001**, *105*, 5546−5552.
(7) Bortolotti, C. A.; Siwko, M. E.; Castellini, E.; Ranieri, A.; Sola, M.; Corni, S. *J. Phys. Chem. Lett.* **2011**, *2*, 1761−1765.
(8) Ly, H. K.; Marti, M. A.; Martin, D. F.; Alvarez-Paggi, D.; Meister, W.; Kranich, A.; Weidinger, I. M.; Hildebrandt, P.; Murgida, D. H. *ChemPhysChem* **2010**, *11*, 1225−1235.
(9) Muegge, I.; Qi, P. X.; Wand, A. J.; Chu, Z. T.; Warshel, A. *J. Phys. Chem. B* **1997**, *101*, 825−836.
(10) Murgida, D. H.; Hildebrandt, P. *Acc. Chem. Res.* **2004**, *37*, 854−861.
(11) Tipmanee, V.; Oberhofer, H.; Park, M.; Kim, K. S.; Blumberger, J. *J. Am. Chem. Soc.* **2010**, *132*, 17032−17040.
(12) Jasaitis, A.; Johansson, M. P.; Wikström, M.; Vos, M. H.; Verkhovsky, M. I. *Proc. Natl. Acad. Sci. U.S.A.* **2007**, *104*, 20811−20814.
(13) Kim, Y. C.; Wikström, M.; Hummer, G. *Proc. Natl. Acad. Sci. U.S.A.* **2009**, *106*, 13707−13712.
(14) Gray, H. B.; Winkler, J. R. *Q. Rev. Biophys.* **2003**, *36*, 341−372.
(15) Basu, G.; Kitao, A.; Kuki, A.; Go, N. *J. Phys. Chem. B* **1998**, *102*, 2085−2094.
(16) Olsson, M. H. M.; Ryde, U.; Roos, B. O. *Protein Sci.* **1998**, *7*, 2659−2668.
(17) Caroppi, P.; Sinibaldi, F.; Fiorucci, L.; Santucci, R. *Curr. Med. Chem.* **2009**, *16*, 4058−4065.
(18) Scott, R. A.; Mauk, A. G. *Cytochrome c: a multidisciplinary approach*; University Science Books: Mill Valley, CA, 1996.
(19) Andrew, S. M.; Thomasson, K. A.; Northrup, S. H. *J. Am. Chem. Soc.* **1993**, *115*, 5516−5521.
(20) Dolidze, T. D.; Rondinini, S.; Verto-Va, A.; Waldeck, D. H.; Khoshtariya, D. E. *Biopolymers* **2007**, *87*, 68−73.
(21) Fedurco, M.; Augustynski, J.; Indiani, C.; Smulevich, G.; Antalik, M.; Bano, M.; Sedlak, E.; Glascock, M. C.; Dawson, J. H. *J. Am. Chem. Soc.* **2005**, *127*, 7638−7646.
(22) Nahir, T. M.; Clark, R. A.; Bowden, E. F. *Anal. Chem.* **1994**, *66*, 2595−2598.
(23) Shafiey, H.; Ghourchian, H.; Mogharrab, N. *Biophys. Chem.* **2008**, *134*, 225−231.
(24) Song, S.; Clark, R. A.; Bowden, E. F.; Tarlov, M. J. *J. Phys. Chem.* **1993**, *97*, 6564−6572.
(25) Terrettaz, S.; Cheng, J.; Miller, C. J. *J. Am. Chem. Soc.* **1996**, *118*, 7857−7858.
(26) Matyushov, D. V. *J. Phys. Chem. B* **2011**, *115*, 10715−10724.
(27) Alvarez-Paggi, D.; Martín, D. F.; DeBiase, P. M.; Hildebrandt, P.; Martí, M. A.; Murgida, D. H. *J. Am. Chem. Soc.* **2010**, *132*, 5769−5778.
(28) Abriata, L. A.; Cassina, A.; Tortora, V.; Marin, M.; Souza, J. M.; Castro, L.; Vila, A. J.; Radi, R. *J. Biol. Chem.* **2009**, *284*, 17−26.
(29) Rumbley, J. N.; Hoang, L.; Englander, S. W. *Biochemistry* **2002**, *41*, 13894−13901.
(30) Murgida, D. H.; Hildebrandt, P. *J. Phys. Chem. B* **2001**, *105*, 1578−1586.
(31) Murgida, D. H.; Hildebrandt, P. *Angew. Chem., Int. Ed.* **2001**, *40*, 728−731.
(32) Murgida, D. H.; Hildebrandt, P. *J. Am. Chem. Soc.* **2001**, *123*, 4062−4068.
(33) Laviron, E. *J. Electroanal. Chem.* **1979**, *101*, 19−28.
(34) Bushnell, G. W.; Louie, G. V.; Brayer, G. D. *J. Mol. Biol.* **1990**, *214*, 585−595.
(35) Rai, B.; Sathish, P.; Malhotra, C. P.; Pradip; Ayappa, K. G. *Langmuir* **2004**, *20*, 3138−3144.
(36) Ying, T.; Wang, Z. H.; Lin, Y. W.; Xie, J.; Tan, X.; Huang, Z. X. *Chem. Commun.* **2009**, 4512−4514.
(37) Berghuis, A. M.; Guillemette, J. G.; McLendon, G.; Sherman, F.; Smith, M.; Brayer, G. D. *J. Mol. Biol.* **1994**, *236*, 786−799.
(38) Luntz, T. L.; Schejter, A.; Garber, E. A.; Margoliash, E. *Proc. Natl. Acad. Sci. U.S.A.* **1989**, *86*, 3524−3528.
(39) Feinberg, B. A.; Petro, L.; Hock, G.; Wenying, Q. I. N.; Margoliash, E. *J. Pharmaceut. Biomed. Anal.* **1999**, *19*, 115−125.
(40) Battistuzzi, G.; Bortolotti, C. A.; Bellei, M.; Di Rocco, G.; Salewski, J.; Hildebrandt, P.; Sola, M. *Biochemistry* **2012**, *51*, 5967−5978.
(41) García-Heredia, J. M.; Díaz-Moreno, I.; Nieto, P. M.; Orzáez, M.; Kocanis, S.; Teixeira, M.; Pérez-Payá, E.; Díaz-Quintana, A.; De la Rosa, M. A. *BBA-Bioenergetics* **2010**, *1797*, 981−993.
(42) Zhou, P.; Tian, F.; Lv, F.; Shang, Z. *Proteins: Struct., Funct. Bioinf.* **2009**, *76*, 151−163.
(43) Blouin, C.; Wallace, C. J. *J. Biol. Chem.* **2001**, *276*, 28814−28818.
(44) Schweitzer-Stenner, R. *J. Phys. Chem. B* **2008**, *112*, 10358−10366.
(45) Murgida, D. H.; Hildebrandt, P. *Chem. Soc. Rev.* **2008**, *37*, 937−945.
(46) Kranich, A.; Ly, H. K.; Hildebrandt, P.; Murgida, D. H. *J. Am. Chem. Soc.* **2008**, *130*, 9844−9848.
(47) Petrovic, J.; Clark, R. A.; Yue, H.; Waldeck, D. H.; Bowden, E. F. *Langmuir* **2005**, *21*, 6308−6316.
(48) Finklea, H. O.; Hanshew, D. D. *J. Am. Chem. Soc.* **1992**, *114*, 3173−3181.
(49) Xu, J.; Li, H.; Zhang, Y. *J. Phys. Chem.* **1993**, *97*, 11497−11500.
(50) Smalley, J. F.; Feldberg, S. W.; Chidsey, C. E. D.; Linford, M. R.; Newton, M. D.; Liu, Y. P. *J. Phys. Chem.* **1995**, *99*, 13141−13149.
(51) Kuznetsov, A. M.; Ulstrup, J. *Electron transfer in chemistry and biology: an introduction to the theory*; Wiley: Chichester, UK, 1999.
(52) Murgida, D. H.; Hildebrandt, P. *J. Phys. Chem. B* **2002**, *106*, 12814−12819.
(53) Monari, S.; Ranieri, A.; Bortolotti, C. A.; Peressini, S.; Tavagnacco, C.; Borsari, M. *Electrochim. Acta* **2011**, *56*, 6925−6931.
(54) Maity, H.; Rumbley, J. N.; Englander, S. W. *Proteins: Struct., Funct. Bioinf.* **2006**, *63*, 349−355.
(55) Kokhan, O.; Wraight, C. A.; Tajkhorshid, E. *Biophys. J.* **2010**, *99*, 2647−2656.
(56) Zhou, J.; Zheng, J.; Jiang, S. *J. Phys. Chem. B* **2004**, *108*, 17418−17424.
(57) Pelletier, H.; Kraut, J. *Science* **1992**, *258*, 1748−1755.
(58) Lange, C.; Hunte, C. *Proc. Natl. Acad. Sci. U.S.A.* **2002**, *99*, 2800−2805.
(59) Roberts, V. A.; Pique, M. E. *J. Biol. Chem.* **1999**, *274*, 38051−38060.
(60) Galinato, M. G. I.; Kleingardner, J. G.; Bowman, S. E. J.; Alp, E. E.; Zhao, J.; Bren, K. L.; Lehnert, N. *Proc. Natl. Acad. Sci. U.S.A.* **2012**, *109*, 8896−8900.

(61) Roberts, V. A.; Pique, M. E. *J. Biol. Chem.* **1999**, *274*, 38051−38060.
(62) Yue, H. J.; Khoshtariya, D.; Waldeck, D. H.; Grochol, J.; Hildebrandt, P.; Murgida, D. H. *J. Phys. Chem. B* **2006**, *110*, 19906−19913.
(63) Blumberger, J. *Phys. Chem. Chem. Phys.* **2008**, *10*, 5651−5667.
(64) Battistuzzi, G.; Borsari, M.; Bortolotti, C. A.; Di Rocco, G.; Ranieri, A.; Sola, M. *J. Phys. Chem. B* **2007**, *111*, 10281−10287.
(65) Takayama, S. J.; Irie, K.; Tai, H. L.; Kawahara, T.; Hirota, S.; Takabe, T.; Alcaraz, L. A.; Donaire, A.; Yamamoto, Y. *J. Biol. Inorg. Chem.* **2009**, *14*, 821−828.
(66) Matsuura, Y.; Takano, T.; Dickerson, R. E. *J. Mol. Biol.* **1982**, *156*, 389−409.
(67) Capdevila, D.; Marmisolle, W.; Williams, F. J.; Murgida, D. H. *Phys. Chem. Chem. Phys.* **2013**, DOI: 10.1039/C2CP42044A.
(68) Abriata, L. A.; Alvarez-Paggi, D.; Ledesma, G.; Blackburn, N. J.; Vila, A. J.; Murgida, D. H. *Proc. Natl. Acad. Sci. U.S.A.* **2012**, *109*, 17348−17353.